A&A 412, L19–L23 (2003)
DOI: 10.1051/0004-6361:20031661

Astronomy & Astrophysics

A new view of dark Martian regions from geomorphic and spectroscopic analysis of Syrtis Major

F. Poulet[1], N. Mangold[2], and S. Erard[1]

[1] Institut d'Astrophysique Spatiale, Université Paris-Sud, 91405 Orsay Cedex, France
[2] Equipe de Géomorphologie Planétaire, Université Paris-Sud, 91405 Orsay Cedex, France

Received 2 September 2003 / Accepted 25 October 2003

Abstract. New analysis of Mars Observer Camera (MOC) images and Thermal Emission Imaging System (THEMIS) data focussed on West Syrtis Major show that this region, usually interpreted as typical of in-situ bedrocks, is covered by a dark mantle which could result from a transient deposition of suspended fine particles still active until a few million years ago. To help address the questions of the nature of these low albedo regions covered by blankets, we revisited the surface composition by modelling Imaging Spectrometer (ISM) spectra with a radiative transfer model, the strength of such a modelling method being to aid in determining appropriate endmembers as well as their relative abundance, their grain size, and the type of mixtures (sand/dust). Two distinct surface compositions (basaltic sand vs. sand/dust mixture of pyroxenes and oxides) are possible. The solution more consistent with the geomorphic analysis is the sand/dust mixture with a large proportion of dusty grains of oxides and/or pyroxenes (about 50–60%). This implies that Type 1 plagioclase-rich lithology derived from Thermal Emission Spectrometer (TES) is not required by NIR data. This work gives new evidence of the presence of dark dust on the surface of Mars.

Key words. planets and satellites: individual: Mars

1. Introduction

Determining a representative crustal composition of Mars would help putting important constraints on thermal history and internal structure, and is a major objective of present and future space missions. Syrtis Major, a low volcanic shield of Hesperian age, is usually presented as characteristic of Martian bedrock, in particular because of its very low albedo and the presence of two small calderas in its center. Early orbital observations in the NIR range (e.g., Erard et al. 1991; Mustard et al. 1993) suggested that the western and central parts of the shield, with marked mafic signatures, have significant exposures of bedrock or locally derived materials. Mustard et al. (1993) interpreted the ISM observations as dominated by augite-bearing basalts and estimated the pyroxene composition. Mustard et al. (1997) derived a two-pyroxenes mineralogy consistent with basaltic SNC meteorites, with the largest fraction of high-calcium pyroxene in the ISM data set observed in West and central Syrtis. Murchie et al. (2000) confirmed that this material is one of the two main endmembers in the ISM data set, the mixture of which describes 80% of the observed regions. Bandfield et al. (2000) and later Hamilton et al. (2001) identified this area as the type region for TES Type 1 dark materials, which is interpreted as basaltic with a composition dominated by plagioclase (50%) and clinopyroxene (20%, mostly augite). Cooper & Mustard (2002) then confirmed a 20% clinopyroxene fraction for TES Type 1 from ISM spectra, and suggested that variations in the visible and near-infrared observations could be controlled by dust or other thermally neutral materials. The aim of the present paper is to study new morphologic evidence provided by MOC and THEMIS high resolution images in the TES Type 1 main area, and to reanalyze ISM spectra of this region using a more quantitative approach.

Send offprint requests to: F. Poulet,
e-mail: francois.poulet@ias.fr

2. Geomorphic analysis

MOC images of West (W) Syrtis Major show a smooth surface texture lacking the features typical of lava flows (Fig. 1A). Large impact craters of several hundred meters have smooth rims and partially filled interiors, and only few impact craters smaller than 100 m are visible. Figure 1B represents all crater size from data available at all scale (MOC to Viking MDIM) plotted over the isochrons defined by Hartmann & Neukum (2001). Craters larger than 1 km follow the isochron of 3 Gy giving the age of the volcanic plain (Hesperian age). This old surface should be saturated of craters smaller than 250 m. However, there is a strong depletion of craters smaller than 500 m. This depletion indicates a resurfacing process that was active until a few million years ago according to isochrons. Recent lava flows are unlikely to explain such depletion

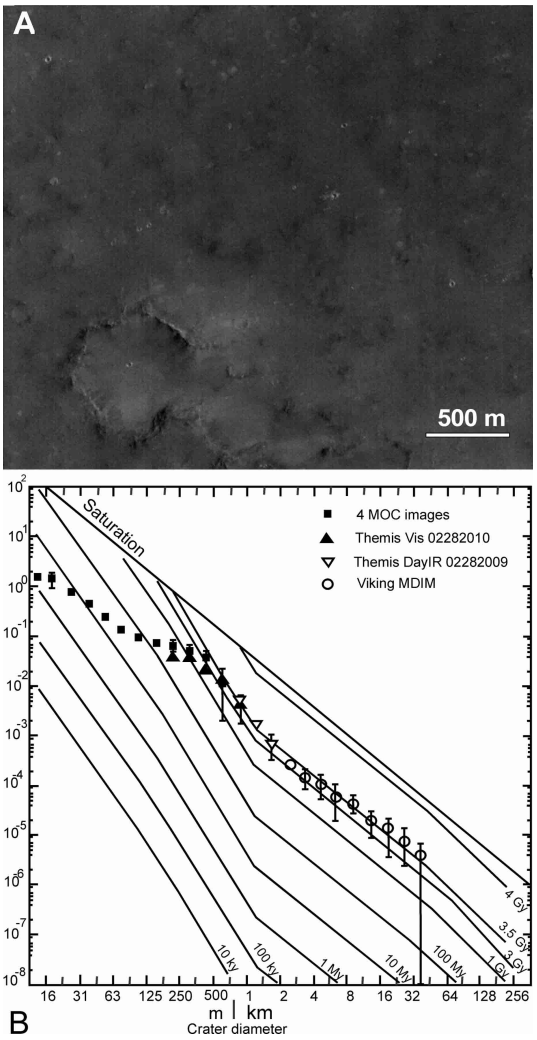

Fig. 1. A) MOC image M08-04241 (MSSS/JPL/NASA) typical of W Syrtis Major. The surface is smooth, the largest craters are partially filled and few small craters are visible. **B)** Crater count of W Syrtis Major over images from MOC to Viking scales. The depletion of craters smaller than 500 m shows the obliteration of small craters by eolian processes.

because flows are punctual episodes which are not able to produce a constant depletion like that observed. On the contrary, such shift of plot from the isochron is typical of progressive resurfacing like observed in Arabia Terra from the deposition of bright dust (Hartmann & Neukum 2001; Vincendon et al. 2002). An eolian filling process is therefore the most likely to explain the smoothness of the surface at the MOC scale (Fig. 1A). According to the rim-to-width ratio of impact craters, the obliteration of craters as large as 500 m implies a minimum thickness of deposits of about 20 m (Vincendon et al. 2002), inconsistent with the assumption of large bedrock exposures in W Syrtis Major.

The non-bedrocky view of the area is further supported by the analysis of thermophysical properties. Mellon et al. (2000) first noted that the low thermal inertia values (180–300 $\mathrm{J\,m^{-2}\,K^{-1}\,s^{-0.5}}$) measured by IRTM and TES in Syrtis are characteristics of fine-grained sand rather than bedrock. THEMIS night IR images are here used to distinguish bedrock

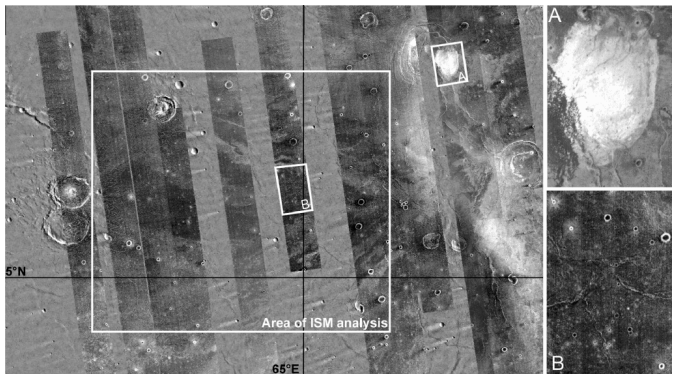

Fig. 2. Mosaic of night-infrared THEMIS images (over Viking MDIM). Bright areas correspond to higher thermal inertia, while dark areas indicate lower thermal inertia. Close-up A shows the caldera of Nili Patera with outcrops of bedrocks and dune fields on the left. Close-up B, over the area analyzed, is devoid of bedrock with exception of the rims of small craters. The area of study corresponds to coordinates 62°E to 67°E and 4°SN to 8°N.

from dust and sand (Fig. 2). On the first order, sand and dust are low thermal inertia materials corresponding to low night temperatures, in contrast to rocks which have higher thermal inertia and display higher night temperatures. According to the mosaic in Fig. 1, bedrock is exposed mainly inside Nili patera (bright area on close-up A) and SW of Meroe patera. By contrast, most of the terrains have a cold nighttime thermal response typical of fine grains, such as the dunes field observed close to Nili patera (gray area at left on close-up A). These "cold" terrains exhibit rocky material only on the flanks of small impact craters or on the ejecta of fresh craters (close-up B). In the box area well covered by THEMIS images (Fig. 2), these outcrops represent strictly less than 5%, showing the predominance of fine grain material.

Edgett & Malin (2000) proposed the occurrence of a dark eolian mantling in parts of Syrtis Major. Since dune fields are not frequent, mantling by deposition of suspended fine particles could explain the smoothness of the surface. Easily removable dust is unlikely because it would produce a thermal inertia lower than observed, while either compacted dust and silt-sized particles, or a mixture of loose silt and sand-sized particles would fit.

The origin of these dark grains is likely the volcanic units of Syrtis Major. However, the original composition of the surface lavas, typically plagioclase/pyroxene/olivine, may have changed significantly during the more than 3 By of surface weathering. The surface may have been submitted to chemical alteration, gardening by small impacts, mechanical disruption by frost and sorting due to wind action which preferentially keep the hardest particles at the surface during time. Moreover, the surface may have been enriched by exogenous particles such as ash deposited from post Syrtis flows activity. The effects of all these processes are not well understood yet, but the consequence is that the final nature and composition of the current mantling is likely different from the original lavas, at least in terms of quantitative proportion of each minerals. The nature and the composition of this blanket are therefore quantitatively

addressed in next section by modelling ISM spectra of W Syrtis Major with a scattering model.

3. Surface composition analysis

3.1. Spectral data

We used fully calibrated ISM data in the Syrtis-Isidis session from the PDS archive on `www.ias.fr/cdp/Base_ISM/INDEX.HTM`. Extra processing includes correction for atmosphering absorption, aerosol scattering and photometric effects, and registration of the two ISM spectral orders. This provides the normal albedo of surface areas ~25 km in size. A smoothed aerosols spectrum is subtracted from the data after scaling its magnitude to the geometry of observation (Erard et al. 1994). A Minnaert function with $k = 0.87$ independent of wavelength is used for the photometric correction. The resulting spectra are characterized by lower albedo, larger spectral contrast in the 1- and 2-μm absorptions, and a change of the spectral slope between 0.8 and 2.5 μm from blue to gray/slightly red.

3.2. Choice of the scattering model

One of the significant challenges to the use of reflectance spectroscopy for quantitative analysis of planetary soil composition is separating the effects of particle sizes from composition. Employing scattering models to explore the extensive parameter space presents the advantage to take into account the influence of grain sizes and all members including spectrally neutral components. The Shkuratov radiative transfer model is here applied for fitting the spectra (Shkuratov et al. 1999). Poulet et al. (2002) showed its degree of realism and of efficiency relative to other scattering models, and in particular to the Hapke model and its derivatives. The model has been also tested to determine the type of mixture (intimate, areal or bedrocky), the relative proportions, and the grain sizes of components of laboratory mineral samples (Poulet & Erard 2003). Finally, the Shkuratov model has an important property: it is invertible, i.e., the spectral absorption coefficient k of a given material can be estimated from reflectance data given the grain size in the sample and a priori knowledge on the real part of refractive index (which may be considered constant in the NIR). Given the optical constants of the endmembers, the model has two free parameters for each endmember: the average grain size and the relative abundance.

3.3. Choice of the endmembers

We selected possible endmembers by trying to satisfy the following characteristics of the spectra: low albedo, shape and depth of the 1- and 2-μm absorptions and spectral slope. Low- and high-calcium pyroxenes were obviously included, as well as olivine. A spectrally featureless low albedo component in the NIR is also required to lower the average spectral reflectance and to reduce the spectral contrast. Oxides such as magnetite display this neutral opaque behavior. Hematite was also considered because of its low albedo and its 0.85 μm absorption. Other minerals such as common amphiboles, obsidians and phyllosilicates were included in some fits. However, they were rejected because they produce prominent OH- and H20- features when present even in very small amount (5%) (Poulet et al. 2003). Some rare very dark high-iron clays wich exhibit bands at 3.0 μm only (Calvin & King 1997) were also tested. Berthierine could be a possible endmember and play the spectral role of the oxide mineral. However, we did not consider such endmembers further because of their rarity. Other common minerals such as plagioclase and olivine were also considered. The optical constants of the possible component are calculated from reflectance spectra in the USGS (Clark et al. 1993) and RELAB librairies, using the inversibility of Shkuratov model. This is discussed and assessed by Poulet & Erard (2003).

3.4. Choice of the end-types of surface and results

The geomorphic analysis shows that the dark blanket which covers large parts of W Syrtis Major can be formed by fine grains rather than coarse grains. Particle size range for dust and drift material on Mars is estimated to be 0.1 to 10 μm (Christensen & Moore 1992). Consequently, submicronic particles (also called dust) are investigated. The three investigated end-types of surface are thus: dust (mixture of particles of size < wavelength λ), sand (intimate mixture of particles of size > λ), dust/sand mixtures. Each ISM spectrum is fit by optimizing the grain sizes and the fractions of endmembers for each type of mixture. The optimization is performed using a downhill simplex procedure (e.g., Press et al. 2002). The two noisiest regions of the spectra ($1.5 < \lambda < 1.7$ and $\lambda > 2.55$ μm) are not taken into account. It must be stressed however that the main limitation of our fits is not related to the signal to noise ratio, but rather to the absolute accuracy of the spectral calibration applied.

Dust-only mixtures provide the less good fits to the spectra, even when a large number of endmembers (up to 9) is considered (Fig. 3A). We therefore discard this solution, although we notice that the fits are marginally acceptable given the absolute accuracy of the data. The observations are best reproduced by a mixture of coarse particles of pyroxenes/hematite/magnetite/olivine/plagioclase. However, large fractions (>50%, Fig. 3B) of hematite or magnetite in very big particles are required to fit the low albedo, which should have been detected by TES (Hamilton et al. 2001). Another solution to lower the albedo is to consider inhomegeneous or "dirty" plagioclase grains containing inclusions of other components such as iron oxide and pyroxene rather than "pure" plagioclase. This type of grains whose scattering properties are calculated by effective medium theories (Bohren & Huffman 1983) can simulate the reflectance spectra of basalts (Poulet & Erard 2003). An example of fit by a mixture of pyroxenes/hematite/olivine/dirty-plagioclase (referred to as basaltic sand) is shown in Fig. 3C. This type of mixture gives residuals only 10% larger in average than our best fit solution (see below) so that it is still considered as an acceptable fit; however, it does includes rather large coarse plagioclase grains, that would probably produce different

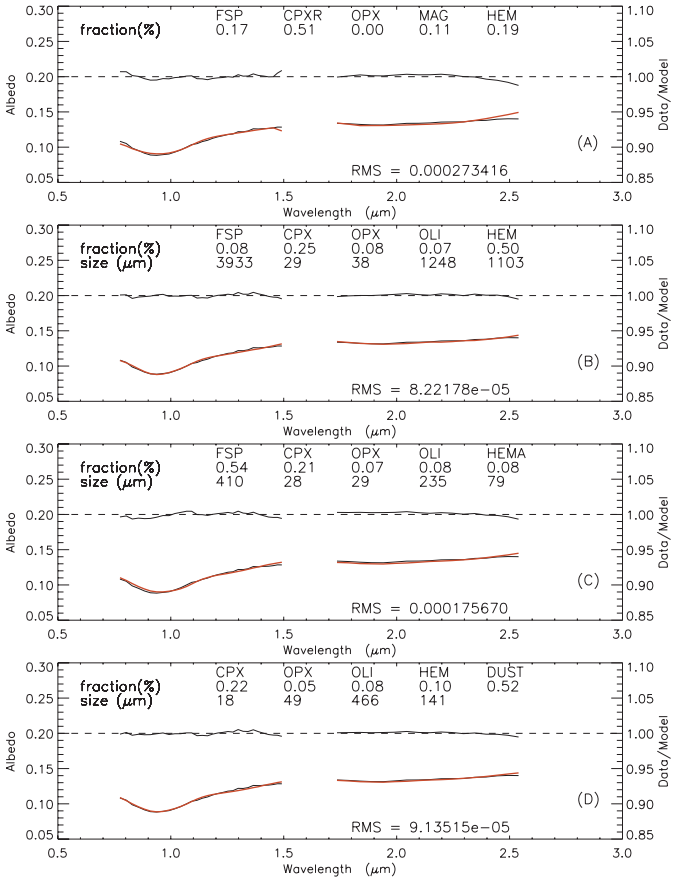

Fig. 3. A representative low albedo spectrum (thick dark line) and four modellings (red line) for different types of mixture: **A)** Dust mixture, **B)** Pure sand mixture, **C)** Basaltic sand, **D)** Sand/dust mixture. The data/model ratio allows a rapid qualitative assesment of the accuracy of each fit. The fraction and average grain size are indicated for the various endmembers, as well as the RMS errors.

surface morphology with sand dune rather than the observed dark blanket. An additional constraint is therefore to fit the spectra with dusty and/or moderate size coarse particles only. Our best fits are actually obtained with a sand/dust mixture (Fig. 3D): a four-component sand mixture of two pyroxenes, olivine, and hematite, and a large fraction (>50%) of a dust phase including magnetite, hematite and/or pyroxene. We outline that both high- and low-calcium pyroxenes (respectively HCP and LCP) are required in the sand. The distribution of fit mixing ratios for these five components in W Syrtis Major shows low dispersions: $12\% \pm 4$, 8 ± 3, 10 ± 1.7, 9 ± 3.7, 63 ± 7 for HCP, LCP, olivine, hematite and dust respectively. That suggests that most ISM pixels there are similar in composition, and covered by homogenized surface materials. The mean grain sizes are 30 ± 14 μm, 24 ± 14, 516 ± 123, 414 ± 139 for the HCP, LCP, olivine, and hematite components respectively. A certain amount of dirty plagioclase may be present instead of coarse hematite and dusty particles but in a proportion smaller than 15%.

4. Discussion and conclusion

Our goal is now to combine the spectral modelling results with the geomorphic analysis. Our spectral study evidences two possible, distinct, surface compositions (basaltic sand or sand/dust mixture), while the smoothness of the Syrtis Major regions studied here is in favor of a dark mantle of several meters in depth resulting from a transient deposition of suspended fine particles. The sand/dust mixture solution (a four-component intimate mixture of LCP, HCP, olivine, and hematite coarse grains mixed with a large proportion of dusty grains of oxides and/or pyroxene), is therefore more consistent with our geomorphic analysis. The other solution which corresponds to a basaltic sand made of large coarse grains only, has the advantage to be consistent with the type-I mineralogy derived from TES data (Bandfield et al. 2000; Hamilton et al. 2001) with pyroxene contents of (~25%) and plagioclase/pyroxene ratios ranged between 1.3–2.4. However, such a mixture would probably produce a different surface morphology with sand dune rather than the observed dark blanket. The solution more consistent with geomorphology thus contains no plagioclase. This does not mean that plagioclase is totally lacking. However, given the lack of spectral features of dirty plagioclase in the NIR range, an upper limit of the abundance of this endmember can be estimated to 10–15%. The possible disconnection between ISM and TES observation modellings could result from the fact that NIR data are much more sensitive to thin coatings than thermal IR data, so that TES data may not detect large amounts of dark dust. However, this explanation is likely uncorrect, because the geomorphic analysis indicates a dark mantle of several meters in depth. The potential lack of basalt with plagioclase/pyroxene >1 is also supported by Minitti et al. (2002) who showed that a plagioclase-rich lithology is not required by the TES data.

Particles sorting of grains is a very efficient process that could modify the proportion of the material of the host rock even without chemical weathering, and result in low plagioclase content. For instance, some volcanic sands in New Zealand contain up to 80% of titanomagnetite (Nicholson & Fyfe 1958). Processes of particle sorting specific to Mars involving long term eolian activity or impact cratering during 3 By could thus have produced such regional enrichment of material. The occurrence in large proportion of magnetite (or titanomagnetite) in the low albedo region of Syrtis is also consistent with the observation of a significant proportion of magnetic grains in brighter regions of Mars like in the landing site of Pathfinder (e.g., Gunnlaugsson et al. 2002). Alternatively, the surface composition derived here may result from regional alteration processes (e.g., Bishop et al. 2002). Finally, this work gives new evidence of the presence of dark mantle of silt sized material on the surface of Mars was already identified by past photopolarimetric, geomorphic and thermophysical observations compiled by Edgett & Malin (2000).

Regarding to our method of analysis, systematically combining geomorphologic, thermophysical properties, NIR spectra and radiative transfer theory to model the spectroscopic results can provide an important incremental step in understanding the composition surface analysis. This procedure will

help clarify rock lithology on Mars from future investigations with forthcoming space missions.

Acknowledgements. We thank S. Fonti for his constructive review.

References

Bandfield, J., Hamilton, V., & Christensen, P. 2000, Science, 287, 1626
Bishop, J. L., Murchie, S., Pieters, M. C., & Zent, A. P. 2002, J. Geophys. Res., 107, E11, 7
Bohren, C. F., & Huffman, H. R. 1983, Absorption and scattering of light by small particles (New-York: Wiley)
Calvin, W. M., & King, T. V. V. 1997, M&PS, 32, 693
Christensen, P. R., & Moore, H. J. 1992, The martian surface layer, in Mars, ed. H. H. Kieffer, B. M. Jakosky, C. W. Snyder, & M. S. Matthews (Tucson: Univ. of Arizona Press)
Clark, R. N., Swayze, G. A., Gallagher, A. J., King, T. V. V., & Calvin, W. 1993, US Geological Survey File, Report 93
Cooper, C. D., & Mustard, J. F. 2002, LPSC, 33, 1873
Edgett, K. S., & Malin, M. C. 2000, J. Geophys. Res., 105, 1623
Erard, S., Bibring, J.-P., Forni, O., Mustard, J. F., & Head, J. W. 1991, LPSC, 21, 437
Erard, S., Mustard, J. F., Murchie, S., et al. 1994, Icarus, 111, 317
Gunnlaugsson, H. P., Weyer, G., & Helgason, O. 2002, Planet. Space Sci., 50, 157
Hamilton, V. E., Wyatt, M. B., McSween, H. Y. Jr., & Christensen, P. R. 2001, J. Geophys. Res., 106, 14733
Hartmann, W. K., & Neukum, G. 2001, Space Sci. Rev., 96, 165
Mellon, M. T., Jakosky, B. M., Kieffer, H. H., & Christensen, P. R. 2000, Icarus, 148, 437
Minitti, M. E., Mustard, J. F., & Rutherford, M. J. 2002, J. Geophys. Res., 107, E5, 6.1
Murchie, S., Kirkland, L., Erard, S., Mustard, J. F., & Robinson, M. 2000, Icarus, 147, 44
Mustard, J. F., Erard, S., Bibring, J.-P., et al. 1993, J. Geophys. Res., 98, 3387
Mustard, J. F., Murchie, S., Erard, S., & Sunshine, J. 1997, J. Geophys. Res., 102, 25 605
Nicholson, D. S., & Fyfe, H. E. 1958, New Zealand J. Geol. Geophys., 19, 153
Poulet, F., Cuzzi, J. N., Cruikshank, D. P., Roush, T., & Dalle Ore, C. M. 2002, Icarus, 160, 313
Poulet, F., & Erard, S. 2003, J. Geophys. Res., submitted
Poulet, F., Erard, S., & Mangold, N. 2003, LPSC, 34, 1691
Press, W. H., Teukolsky, S. A., Vetterling, W. T., & Flannery, B. P. 2002, Numerical Recipes in C++ (Cambridge: Cambridge Univ. Press)
Shkuratov, Y., Starukhina, L., Hoffmann, H., & Arnold, G. 1999, Icarus, 137, 235
Vincendon, C., Mangold, N., Masson, P., & Ansan, V. 2002, LPSC, 33, 1208